Turkish Journal of Agriculture and Forestry

Volume 48 | Number 2 Article 12

4-1-2024

Antioxidant Properties and Aldose Reductase Inhibitory Potency of Viscum album L. Extracts: Experimental and Computational Insights

Bilal Akyüz

Bülent Şengül

TÜBİTAK

Turkish Journal of Agriculture and Forestry

http://journals.tubitak.gov.tr/agriculture/

Research Article

Turk J Agric For
(2024) 48: 305-316

doi:10.55730/1300-011X.3182

Antioxidant properties and aldose reductase inhibitory potency of *Viscum album* L. extracts: experimental and computational insights

Bilal AKYÜZ[1], **Bülent ŞENGÜL**[2,*]

[1]Department of Chemistry, Graduate School, Bayburt University, Bayburt, Turkiye
[2]Department of Health Care Services, Vocational School of Health Services, Bayburt University, Bayburt, Turkiye

Received: 28.08.2023 • **Accepted/Published Online:** 07.02.2024 • **Final Version:** 01.04.2024

Abstract: This study systematically investigates the antioxidant capacity and inhibitory impact of *Viscum album* L. plant extracts on the aldose reductase (AR) enzyme through a combined approach of in vitro and in silico methods. Various sections derived from distinct plant parts were examined, revealing potent inhibitory potential. Notably, the methanol extract sourced from the plant's stem displayed remarkable efficacy with an IC_{50} value of 0.156 µM. Total phenolic content and antioxidant capacity analyses were conducted, highlighting variations across plant parts and solvent types. Qualitative and quantitative phenolic compound content in the extracts was elucidated by LC-MS/MS analysis, revealing higher levels of quinic acid, fumaric acid, and chlorogenic acid. Molecular docking studies further substantiated the inhibitory roles of key compounds like chlorogenic acid and fumaric acid, elucidating their interactions with specific amino acid residues within the AR enzyme's active site and shedding light on the underlying mechanisms. Collectively, this study underscores *Viscum album* L. extracts as promising candidates for aldose reductase modulation. By merging experimental and computational techniques, the study presents a holistic understanding of natural compound interactions, potentially influencing drug development and herbal therapeutics.

Key words: *Viscum album* L., aldose reductase, herbal medicine, diabetic complications

1. Introduction

Diabetes mellitus, characterized by elevated blood glucose levels, is a chronic metabolic disorder that has become a global health concern due to its increasing prevalence and associated complications (Kousaxidis et al. 2020, Şengül 2023). Chronic hyperglycemia, a fundamental feature of diabetes mellitus, can lead to a range of serious complications over the long term. While these complications constitute a critical component of diabetes management and treatment, they can significantly impact patients' quality of life (Alim et al. 2017b, Singh et al. 2021). The long-term effects of diabetes stem from the disruption of metabolic pathways caused by elevated blood sugar levels. One such pathway is the polyol pathway, a series of biochemical reactions primarily involving the enzyme aldose reductase (Şengül and Beydemir 2018, Kılınç 2021, Thakur et al. 2021). In recent years, research investigating the effects of natural plants and herbal compounds on diabetes complications has gained momentum. In this context, *Viscum album* L. (mistletoe) is considered one of the plants that could potentially have positive effects on the polyol pathway and aldose reductase activity through its bioactive components (Orhan et al. 2005, Ullah et al. 2022).

The mechanisms underlying diabetes complications are complex and multifaceted. One of these complications is the activation of the polyol pathway resulting from hyperglycemia. The key components of the polyol pathway involve the conversion of glucose to aldose through the enzyme aldose reductase, followed by the reduction of aldose to sorbitol and fructose. This process can occur at an accelerated rate in glucose-sensitive tissues such as the retina, kidneys, and peripheral nerves. The role played by aldose reductase along this pathway has significant implications for the pathogenesis of microvascular complications of diabetes. Increased sorbitol production due to hyperglycemia can lead to impaired cellular osmosis, increased oxidative stress, and ultimately cellular damage. This mechanism is considered one of the factors underlying diabetic retinopathy, nephropathy, and neuropathy (Alim et al. 2017a, Balestri et al. 2022)

Traditional medicine suggests that natural herbal sources could potentially play a role in managing diabetes and its associated complications. *Viscum album* L. (Mistletoe) is one such herbal compound that stands out in this context. *Viscum album* L. contains a variety of bioactive components, including lectins,

* Correspondence: bulentsengul@bayburt.edu.tr

viscotoxins, amino acids, flavonoids, phenylpropanoids, triterpenes, phytosterols, alkaloids, polyalcohols, and polysaccharides. Some studies suggest that *Viscum album* L. can inhibit aldose reductase activity, thereby blocking the polyol pathway and potentially reducing the long-term complications of diabetes. Particularly, the antioxidant and antiinflammatory properties of *Viscum album* L. could mitigate the effects of oxidative stress and inflammation caused by diabetes (Üstüner 2019, Korcan et al. 2023).

This study examines the potential effects of *Viscum album* L. on the polyol pathway and aldose reductase activity in diabetic complications. Specifically, it investigates how the components of *Viscum album* L. could modulate the polyol pathway and prevent the development of diabetes complications. The findings of this study could contribute to the development of new strategies for the treatment and management of diabetes and its complications.

2. Materials and methods

2.1. Aldose reductase (AR) purification

The purification of AR was conducted using the method described in our previous research (Alim et al. 2017b). All purification experiments were conducted at a temperature of +4 °C.

2.2. Aldose reductase activity assay

AR activity was assessed by monitoring the change in absorbance of NADPH at 340 nm using a spectrophotometer. The enzymatic reaction mixture, with a total volume of 1 mL, comprised 0.8 M Na-phosphate buffer (pH 5.5), 4.7 mM DL-glyceraldehyde, 0.11 mM NADPH, and the enzyme solution. An enzyme unit is defined as the amount of enzyme required to consume 1 µmol of NADPH per minute (Cerelli et al. 1986).

2.3. Collection of plant material

Viscum album L. was collected at the flowering stage from the yellow pine forests of Ormanağzı Village, Olur District, Erzurum Province in September. The taxonomic identification of the plant materials was confirmed by a senior plant taxonomist, Meryem Şengül Köseoğlu, at the Department of Biology, Atatürk University, Erzurum. The collected plant materials were dried in the shade, and the leaves were separated from the stems.

2.4. Extracts preparation

Dried fruit, leaf, and stem samples of the *Viscum album* L. plant were prepared for analysis by grinding under suitable conditions. The extraction process was performed using three different solvents: ethanol, methanol, and water, each with varying polarities. Initially, 5 g of weighed samples were mixed with 100 mL of solvent and shaken at 125 rpm, at a temperature not exceeding 37 °C, overnight in an orbital shaker incubator. Subsequently, the samples were purified from plant materials using filter paper. To remove the solvent from the obtained filtrate, evaporation was conducted under vacuum at a temperature not exceeding 37 °C. The resulting extracts were stored at –20 °C for further studies.

2.5. In vitro inhibition studies

In inhibition experiments, AR activity was assayed as described in Section 2.2. Initially, stock solutions of the extracts were prepared at a concentration of 1 mg/mL. AR activity was quantified by employing various concentrations of *Viscum album* L. extracts. A control sample without an inhibitor was accepted as 100% activity, and activities in the presence of the extract were calculated as a percentage of this control activity. Subsequently, graphs illustrating the percentage of AR enzyme activity versus the concentration of *Viscum album* L. extract for each tissue were generated. The IC_{50} values were calculated from the equations of these graphs.

2.6. Determination of total phenolic contents

The total phenolic content (TPC) of ethanol, methanol, and aqueous extracts prepared from the fruit, leaf, and stem parts of *Viscum album L.* plant was determined using the Folin-Ciocalteu reagent (FCR assay), following the method developed by Slinkard and Singleton (1977). Gallic acid (GA) at a concentration of 1 mg/mL was used as the standard phenolic compound. The TPC values of the extracts were calculated as milligrams of gallic acid equivalent per gram of dried extract (mg GAE/g dried extract).

2.7. Cupric ions (Cu^{2+})-reducing power-CUPRAC assay

The Cu^{2+} ions (cupric ions) were employed as a secondary method to assess the reducing ability of *Viscum album* L. extracts. The Cu^{2+}-reducing ability was evaluated following a slightly modified version of the procedure outlined by Apak et al. (2004). In this method, 0.25 mL of a $CuCl_2$ solution (0.01 M), 0.25 mL of an ethanolic neocuproine solution (7.5×10^{-3} M), and 0.25 mL of an NH_4OAc buffer solution (1 M) were mixed in a test tube with varying concentrations of *Viscum album* L. extracts (ranging from 10 to 30 mg/mL). The total volume was adjusted to 2 mL with distilled H_2O and vigorously shaken. After 30 min, the absorbance of the samples was measured at 450 nm (Çakır and Karabulut 2020).

2.8. DPPH· (2,2-diphenyl-1-picrylhydrazyl) radical scavenging activity

The DPPH· radical scavenging activity of *Viscum album* L. extracts was determined following the method described by Brand-Williams et al. (1995). The prepared extracts were thoroughly mixed and incubated in a dark environment for 30 min. Subsequently, the absorbance value at 517 nm was measured using a spectrophotometer (Güller et al. 2021).

2.9. Ferric reducing antioxidant power (FRAP)

In this method, the FRAP reagent was prepared by mixing, just before use, a solution containing 10 mM acetate buffer

(pH 3.6), 10 mM 2,4,6-tripyridyl-s-triazine (TPTZ), and 20 mM $FeCl_3 \cdot 6H_2O$ in a 10:1:1 ratio. The diluted samples were then mixed with 2 mL of the FRAP reagent and incubated in the dark for 30 min. Subsequently, their absorbance was measured at 593 nm. The results were expressed in Trolox equivalents (TE) (Upadhyay et al. 2010, Kumlay et al. 2021).

2.10. LC-MS/MS analysis

In the LC-MS/MS system, a Zorbax SB C18 column (100 mm L × 4.6 mm ID, 3.5 µm dp) from Agilent Technologies, MA, USA, was utilized. The column oven temperature was set to 30 °C. The flow rate was adjusted to 0.4 mL/min, and the total run time was 20 min. Water containing 0.1% (v/v) formic acid served as phase A, while acetonitrile containing 0.1% (v/v) formic acid was used as phase B for the mobile phase. The elution profile was as follows: from 0.00 to 4.00 min, 5% Mobile Phase B; from 4.01 to 7.00 min, 20% Mobile Phase B; from 7.01 to 14.00 min, 90% Mobile Phase B; from 14.01 to 15.00 min, 90% Mobile Phase B; after 15.10 min, 5% Mobile Phase B. To prepare the 100 mg methanol extracts, each sample was dissolved in 1 mL of methanol. For the 100 mg water extracts, each sample was dissolved in 1 mL of water using vortex and ultrasonic bath assistance. The final solution was transferred to an automated sample vial using a 0.45-micron syringe tip filter. A 5-µL sample was injected into the LC-MS/MS system for analysis. Samples in the autosampler were maintained at 5 °C throughout the experiment.

2.11. Molecular docking

In silico investigations were conducted to explore the interaction between compounds in *Viscum album* L. extracts and the AR enzyme through molecular docking simulations utilizing the Induced-Fit approach, as outlined in previous research (Akıncıoğlu et al. 2021, Gök et al. 2021, Kılınç et al. 2022a, Kılınç et al. 2022b, Şenol et al. 2023a). These simulations were conducted using Maestro 12.5, a component of the Schrödinger Molecular Modeling Suite software (Şenol et al. 2023b). The crystal structure of the AR enzyme, identified by PDB ID: 2FZD, was obtained from the RCSB Protein Data Bank. The enzyme structure was prepared at physiologically relevant pH using the Protein Preparation Wizard (Sastry et al. 2013). The optimization and minimization of the enzyme structure was performed employing the OPLS3e force field. Subsequently, a receptor grid was generated around the natural ligand present in the protein structure. The ligands were processed and protonated at a pH of 7.0 ± 2.0 utilizing the LigPrep module (Tokalı et al. 2023a).

2.12. Calculation of binding free energy using molecular mechanics/generalized born surface area (MM-GBSA)

Binding free energy calculations were performed using the molecular mechanics/generalized born surface area (MM/GBSA) method. This approach integrates continuum solvation models with molecular mechanics computations to estimate the binding free energies of protein-ligand complexes. Prime/MM-GBSA calculations utilized the OPLS3e force field and the VSGB solvation model (Genheden and Ryde 2015, Şenol et al. 2023d).

2.13. Molecular dynamics simulations

Molecular dynamics simulations were conducted using the Desmond software from D. E. Shaw Research. Based on the results of molecular docking and molecular mechanics, the quinic acid-AR complex with the highest score and free binding energy was selected. The protein-ligand complex was prepared using the Desmond system builder module and positioned at the center of an orthorhombic box with a 10 Å buffer zone surrounding the protein. The system was solvated and neutralized by incorporating water molecules (Tip3p) and counter ions (NaCl at 0.15 M). Energy minimization was performed employing the OPLS3 force field. The complex was then subjected to a 100 ns molecular dynamics simulation under consistent temperature (300 K) and pressure (1 bar) conditions, utilizing default parameters. The simulation employed a time step of 2.5 fs and the RESPA integrator. Interactions between the ligand and protein during binding were analyzed, and root mean square deviation (RMSD) for the protein's Cα atoms and the ligand's heavy atoms were computed using Desmond (Şenol et al. 2023c, Şenol et al. 2023d, Tokalı et al. 2023b).

3. Results and discussion

In this study, extracts were prepared from different parts of *Viscum album* L. (mistletoe) plants growing on pine trees in the Sarıçam forests of Ormanağzı Village, located in the Olur District of Erzurum, using various solvents. The prepared extracts were subjected to analyses to determine their total phenolic content, antioxidant capacity, and in vitro and in silico aldose reductase enzyme inhibition studies. We evaluated the inhibitory effects of ethanolic, methanolic, and aqueous extracts prepared from the fruit part of *Viscum album* L. (mistletoe) on AR enzyme activity, revealing IC_{50} values of 1.174 µg/mL, 0.860 µg/mL, and 1.560 µg/mL, respectively. Additionally, extracts derived from the leaf part of *Viscum album* L. were tested, resulting in IC_{50} values for ethanolic, methanolic, and aqueous extracts of 1.090 µg/mL, 0.190 µg/mL, and 9.260 µg/mL, respectively. Moreover, the stem part of *Viscum album* L. was investigated, leading to IC_{50} values for ethanolic, methanolic, and aqueous extracts of 0.700 µg/mL, 0.153 µg/mL, and 0.906 µg/mL, respectively.

These findings highlight the methanol extract prepared from the stem part of *Viscum album* L. as displaying the most potent inhibitory effect on the AR enzyme, with an IC_{50} value of 0.156 µM. The variation in inhibitory potencies among the different plant parts and solvent

types might be attributed to the varying compositions of bioactive compounds within the extracts. Notably, quinic acid emerged as the predominant constituent within the methanol extract derived from the botanical stem segment. Impressively, this particular extract has exhibited remarkable efficacy in inhibiting the activity of the AR enzyme. Given quinic acid's established prominence as a potent inhibitor of the AR enzyme, a characteristic that has been substantiated through a multitude of rigorous scientific investigations (Cui et al. 2009, Veeresham et al. 2014), this observation holds significant importance.

Furthermore, the aqueous extracts of the stem part of *Viscum album* L. plant, which exhibited high inhibition of the AR enzyme, were found to contain a substantial amount of fumaric acid (Table 1). This suggests that fumaric acid compound may be responsible for the observed inhibition of the AR enzyme by the aqueous extract of the plant. Additionally, chlorogenic acid, another constituent detected in notable abundance within extracts derived from *Viscum album* L. plant, is recognized for its robust AR enzyme inhibitory potency, is chlorogenic acid. The current assessment postulates that one of the contributing agents accountable for the observed inhibition of the androgen receptor (AR) enzyme within these extracts is the compound in question. This proposition is supported by a substantial body of scientific literature, wherein numerous investigations have consistently demonstrated the efficacy of chlorogenic acid as a proficient AR inhibitor (de la Fuente and Manzanaro 2003, Paek et al. 2013, Alim et al. 2017a).

Table 1. Phenolic compound content of *Viscum album* L. plant.

Phenolic compound	***Viscum album* L.** (µg/g dw)								
	Fruit			**Leaf**			**Stem**		
	EtOH	**MeOH**	**Aqueous**	**EtOH**	**MeOH**	**Aqueous**	**EtOH**	**MeOH**	**Aqueous**
Quinic acid	17.76	16.14	8.66	51.84	64.97	33.71	113.92	110.73	74.85
Fumaric acid	0.16	3.89	37.12	0.36	1.84	16.82	0.42	1.91	15.71
Cyanidin-3-o glucoside	0.91	0.63	0.46	1.19	0.45	0.15	0.39	0.12	0.02
Chlorogenic acid	22.79	27.71	0.31	29.06	49.05	0.17	28.56	43.76	0.13
Caffeic acid	0.26	nd	nd	nd	nd	nd	nd	nd	nd
Vanillic acid	nd	0.04	0.23	nd	0.03	nd	nd	nd	nd
p-Coumaric acid	0.02	0.01	nd	0.02	0.01	nd	nd	nd	nd
Sinapic acid	0.40	0.23	nd	0.16	0.08	nd	0.06	nd	nd
Taxifolin	nd	nd	nd	0.31	nd	nd	nd	nd	nd
Ferulic acid	0.50	0.27	0.27	0.06	nd	nd	nd	nd	nd
Rosmarinic acid	0.03	nd	nd	0.03	nd	nd	0.04	nd	nd
Myricetin	nd	nd	nd	0.10	nd	nd	nd	nd	nd
Quercetin	0.13	0.12	0.09	0.32	0.10	0.26	0.01	nd	0.23
Naringenin	1.00	0.84	0.67	5.80	2.10	1.52	1.78	0.17	1.13
Isorhamnetin	0.04	0.05	nd	0.30	0.49	nd	nd	nd	nd

nd: not detected

The determination of the total phenolic content of *Viscum album* L. was conducted using the Folin–Coicalteu method, and the obtained results are presented in Table 2. As shown in Figure 1A, the highest total phenolic content was observed in the methanol extract prepared from the fruit part of the plant (5.511 ± 3.679 mg GAE/L extract). Furthermore, the total phenolic content in the methanol extracts of the plant's leaf and stem parts was also higher compared to the other two solvents, measuring 4.48 ± 2.39 mg GAE/g dry extract and 4.56 ± 0.99 mg GAE/g dry extract, respectively.

In a study conducted by Ergün (2021), the total phenolic content in the buds and leaves of *V. album* ssp. *austriacum* collected from pine trees was determined to be 16.88 ± 2.77 mg GAE/g and 19.55 ± 4.68 mg GAE/g, respectively. Yıldız et al. (2019) reported a total phenolic content value of 6.114 mg GAE/g in the methanol extracts of mistletoe growing on Scots pine (*P. sylvestris*). In another study conducted on mistletoe growing on pear and poplar trees, the total phenolic content values were reported as 9.589 mg GAE/g and 9.504 mg GAE/g, respectively (Yıldız et al. 2021).

Methanol extracts of *Viscum album* L. growing on different trees (*Fraxinus pensylvanica* Marsh., *Fraxinus pensylvanica* M., *Sorbus aucuparia* L., *Populus nigra* 'Italica' L., *Tilia cordata* Mill.) were found to contain the following amounts of phenolic compounds: 8.82 ± 0.18, 6.71 ± 0.32, 9.66 ± 0.28, 10.43 ± 0.20, 4.78 ± 0.09 mg GAE/g dry extract, respectively (Pietrzak et al. 2017).

The *Viscum album* L. samples used in our study were grown on pine trees. When compared to existing literature data, the phenolic content of our samples aligns with findings from studies conducted on both the same and different host trees. The slight variations in our results are attributed to the influence of the host tree and the region in which the plant was grown on the phenolic content of the plant.

In our study, the DPPH method was employed to determine the antiradical effects of *V. album* extracts, and the results obtained are presented as percentage inhibition values in Table 2. Although the percentage inhibition values obtained for all parts of the plant were quite close for all solvents in the DPPH analysis, the percentage inhibition values obtained for the methanol extracts were higher compared to the other two solvents. The percentage inhibition values for the methanol extracts prepared from the fruit, leaf, and stem parts of the plant were found to be 91.35 ± 0.14, 87.86 ± 0.20, and 88.87 ± 0.19, respectively.

Upon examining the percentage inhibition values, it can be stated that the methanol extract prepared from the fruit part of the plant exhibited a notably high value of 91.35 ± 0.14 (Figure 1B). In our study, the percentage inhibition values for *V. album* grown on pine trees, considering all parts of the plant, ranged from 72.51 to 91.35. In a study conducted by Köse et al. (2020) on *V. album* grown on pear trees, the DPPH analysis resulted in percentage inhibition values ranging from 47.12 to 30.39. In another study, ÖnayUçar et al. (2006) determined that the DPPH radical scavenging percentage inhibition values for methanol extracts of mistletoes grown on different trees ranged from 59.52 to 95.12. Önay (2002) found percentage inhibition values in the range of 73.44–95.12 for *Viscum album* extracts grown on different host trees in their DPPH analysis. Karaaslan (2020) observed percentage inhibition values in the ranges of 67.30–87.52, 79.00–89.59, and 84.68–91.74 for the extracts prepared from the fruit, leaf, and stem parts of *V. album* plants grown at different altitudes and on different host trees ranging from 980 to 1450 m.

In another antioxidant capacity determination method, the CUPRAC analysis yielded results presented in Table 2 as mg TE/g. According to our findings, the aqueous extract prepared from the leaf part of the plant exhibited the highest activity, with a value of 87.84 ± 0.23 mg TE/g, as illustrated in Figure 1C. However, the Trolox equivalent of the methanol extracts from the fruit and stem parts of the plant surpassed that of the other two solvents. These extracts were determined to have Trolox equivalents of 45.59 ± 0.30 and 74.29 ± 0.30 mg TE/g, respectively.

Additionally, antioxidant capacity was assessed using the ferric reducing antioxidant power (FRAP) method, and the results are shown in Table 2 as μmol $FeSO_4.7H_2O$/g. According to our findings displayed in Figure 1D, the methanol extract prepared from the stem part of the plant exhibited the highest antioxidant capacity (90.02 ± 22.87 μmol $FeSO_4.7H_2O$/g). Similarly, the methanol extract prepared from the fruit part of the plant showed higher antioxidant capacity (62.61 ± 10.38 μmol $FeSO_4.7H_2O$/g) compared to the other solvents, while the aqueous extract from the leaf part of the plant demonstrated a higher antioxidant capacity (75.17 ± 12.79 μmol $FeSO_4.7H_2O$/g) compared to the other solvents. In a study by Yıldız et al. (2019) using the same method, they determined the antioxidant capacity for *U. filipendula* and *V. album* as 54.4 and 51.45 μmol $FeSO_4.7H_2O$/g, respectively.

Induced-fit docking (IFD) investigations were additionally conducted to illuminate the binding mechanisms inherent to the compounds quinic acid, chlorogenic acid, and fumaric acid. These compounds, believed to underlie the inhibition of the aldose reductase (AR) enzyme, were detected in notable concentrations within the *Viscum album* L. plant extracts. These extracts have exhibited potent inhibitory prowess against the AR enzyme. Furthermore, the Prime MM/GBSA module was employed to quantitatively assess the binding energies to gain a comprehensive understanding of the

Table 2. Total phenolic content and antioxidant properties of *Viscum album* L. extracts.

Plant	Parts	Extract type	Total phenolic content (mg GAE/g) ± SD	DPPH %inhibition ± SD	CUPRAC (mg TE/g) ± SD	FRAP (µmol $FeSO_4.7H_2O$/g) ± SD
V. album L.	Fruit	EtOH	4.25 ± 2.44	83.7 ± 0.28	24.61 ± 0.23	25.87 ± 1.64
		MeOH	5.51 ± 3.67	91.35 ± 0.14	45.59 ± 0.30	62.61 ± 1.03
		Aqueous	3.88 ± 3.37	81.95 ± 0.31	27.76 ± 1.29	30.73 ± 3.36
	Leaf	EtOH	4.27 ± 2.65	82.34 ± 0.29	22.22 ± 0.21	34.17 ± 7.39
		MeOH	4.48 ± 2.39	87.86 ± 0.20	63.11 ± 0.33	66.02 ± 6.01
		Aqueous	3.80 ± 0.59	76.00 ± 0.42	87.84 ± 0.23	75.17 ± 12.79
	Stem	EtOH	4.15 ± 1.22	85.97 ± 0.24	41.56 ± 0.40	46.67 ± 11.73
		MeOH	4.56 ± 0.99	88.87 ± 0.19	74.29 ± 0.30	90.02 ± 22.87
		Aqueous	3.06 ± 1.85	72.51 ± 0.48	41.32 ± 0.21	30.31 ± 5.87

*SD: standard deviation.

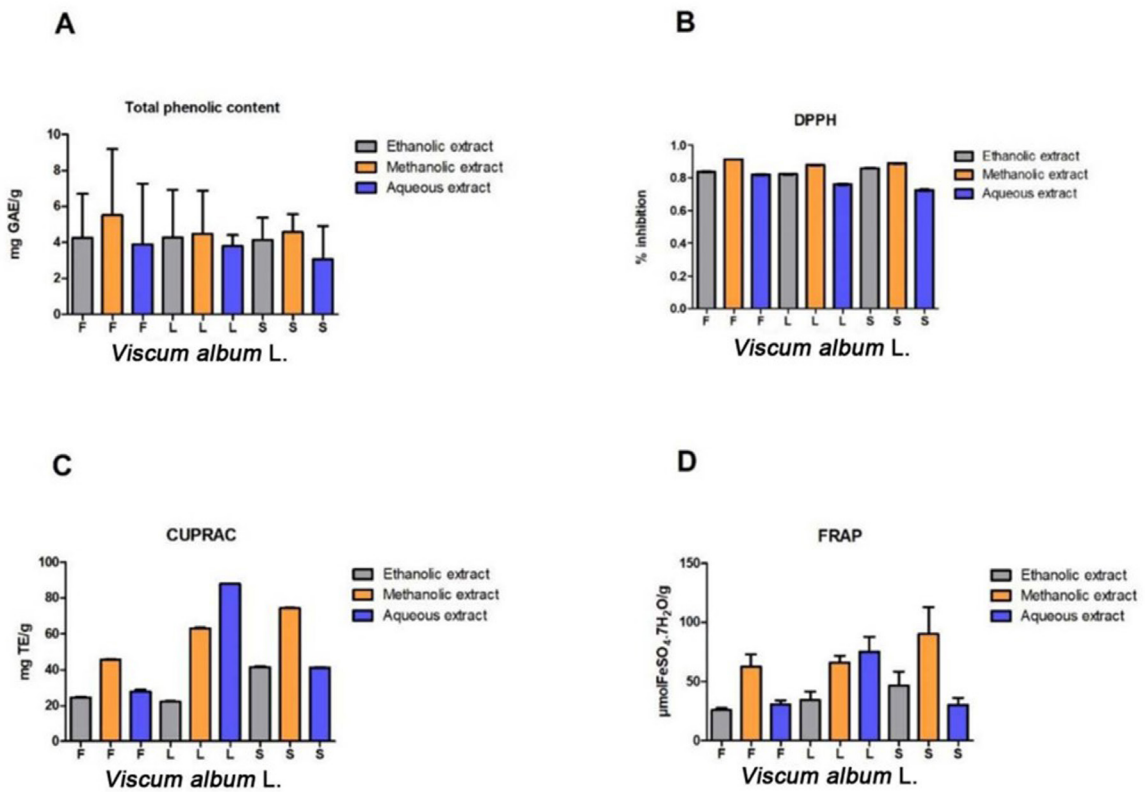

Figure 1. Antioxidant capacity of *Viscum album* L. extracts: (a) TPC: total phenolic content by gallic acid equivalents. (b) DPPH: 1,1-diphenyl-2- picrylhydrazyl by Trolox equivalents. (c) CUPRAC: cupric ion reducing antioxidant capacity. (d) FRAP: ferric reducing antioxidant power by Trolox equivalents.
*F: fruit; L: leaf; S: stem.

thermodynamic factors implicated in the inhibitory mechanisms of quinic acid, chlorogenic acid, and fumaric acid on the AR enzyme. The comprehensive analysis of this data is presented in Table 3, which outlines the IFD docking scores alongside the corresponding Prime/MM-GBSA values.

In the realm of molecular docking investigations involving compounds abundantly present in *Viscum album* L. plant extracts, the compound chlorogenic acid demonstrated the most favorable binding affinity, manifesting a remarkable docking score of –14.092 kcal/mol alongside a corresponding free binding energy of –76.20 kcal/mol (Table 3).

Chlorogenic acid established hydrogen bonding interactions with distinct amino acid residues, specifically Hie-110, Trp-111, Asn-160, Gln-183, and Ser-302. Furthermore, a salt bridge interaction was observed between chlorogenic acid and Lys-77. The 2D ligand-protein interactions between the AR enzyme and chlorogenic acid are depicted in Figure 2A. On the other hand, in the catalytic site of the AR enzyme, fumaric acid formed hydrogen bond interactions with different amino acid residues, particularly Tyr-48, Lys-77, Hie-110, Asn-160, Ser-159, and Gln-183. The 2D ligand-protein interactions between the AR enzyme and fumaric acid are also illustrated in Figure 2B.

Quinic acid was found to be the most abundant secondary metabolite in *Viscum album* L. plant extracts. Within the catalytic site of the AR enzyme, quinic acid engaged in hydrogen bonding interactions with particular amino acid residues, notably Tyr-48, Hie-110, Trp-111, Tyr-209, and Cys-298. The comprehensive 3D docking pose (left side of Figure 3), along with the corresponding 2D diagram illustrating the interactions between the ligand and receptor (depicted on the right), pertaining to quinic acid's configuration in relation to the AR enzyme, is presented in Figure 3.

Molecular dynamics (MD) investigations were conducted to assess the stability of the ligand-protein complex of quinic acid (QA) and aldose reductase (AR) enzyme based on previously published studies (Şenol et al. 2023a, Şenol et al. 2023c, Şenol et al. 2023d, Tokalı

Table 3. IFD docking scores, and Prime/MM-GBSA free binding energy results of the phenolic compounds found in high amounts in the *Viscum album* L. plant.

	Aldose reductase (PDB ID: 2FZD)	
Compound	**IFD docking score (kcal/mol)**	**MM-GBSA ΔG_{bind} (kcal/mol)**
Chlorogenic acid	–14.092	–76.20
Quinic acid	–8.548	–45.97
Fumaric acid	–5.380	–23.16

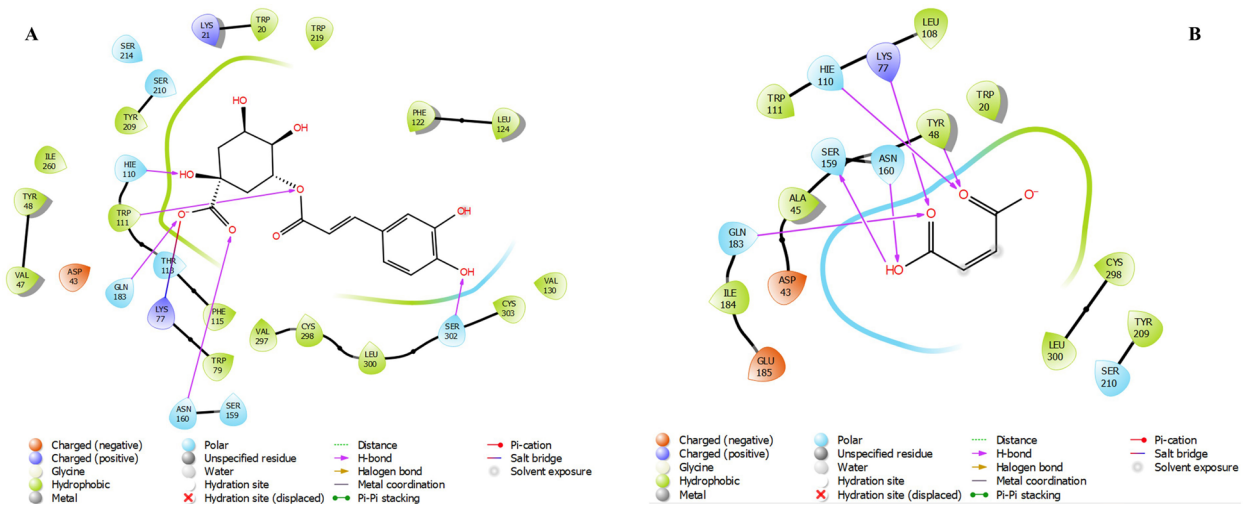

Figure 2. The 2D ligand-protein interactions between AR enzyme and chlorogenic acid (A) and fumaric acid (B).

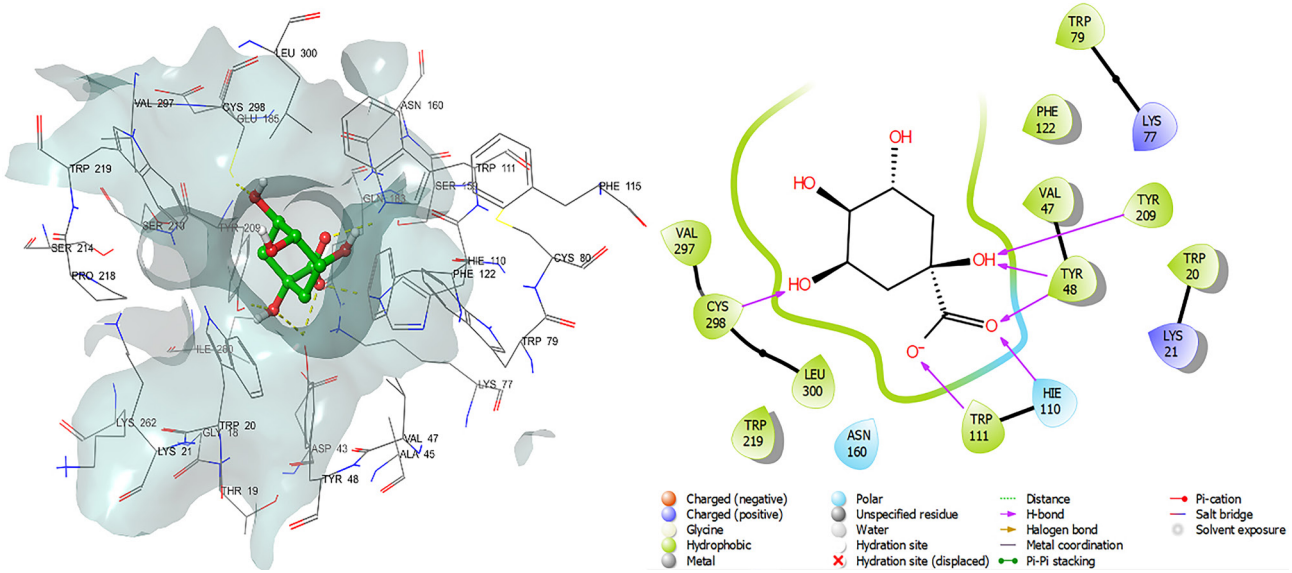

Figure 3. The 3D (left) and 2D (right) ligand-protein interactions between AR enzyme and quinic acid.

et al. 2023a, Tokalı et al. 2023b). This approach involved simulating the dynamic behavior of the complexes over a specific period. As part of the analysis, root-mean-square deviation (RMSD) values were computed for both the ligand atoms and the protein structure. The RMSD values serve as indicators of the fluctuations and deviations in atomic positions throughout the simulation.

By performing these MD simulations and calculating RMSD values, the research aimed to gain insights into the overall stability of the QA-AR complex. These analyses provide a comprehensive understanding of how the complex's components interact and how they undergo structural changes over time. The obtained data aids in assessing the binding strength, potential conformational changes, and overall reliability of the ligand-protein interaction.

The 100 ns MD simulation analysis of the QA-AR complex is depicted in Figures 4 and 5, while Figure 3 presents the key interactions observed during the MD simulation of the related complex. Additionally, Figure 4 presents the RMSD values and MD interaction fraction histograms of the related complex.

As depicted in Figure 4A, the QA formed three different direct hydrogen bond interactions with Trp-111 (58% of simulation time), Tyr-209 (57% of sim.), and His-110 (60% of sim.). Additionally, QA formed three different water-bridged hydrogen bond interactions with Asn-160 (42% of sim.), Tyr-48 (21% of sim.), and Lys-77 (43% of sim.). Interestingly, an intramolecular hydrogen bond interaction was observed between the carboxylic acid and the 1,3-cis positioned OH group during 81% of the simulation time.

Figure 4B presents a pose obtained from 3D interactions of the QA-AR complex during MD simulations. In Figure 4B, the yellow dashes represent the hydrogen bond interactions between QA and the amino acid residues of AR. All hydrogen bond lengths were measured and evaluated, ranging from 2.58 Å to 3.19 Å. These values provide crucial information about the distances between the interacting hydrogen and acceptor atoms, elucidating the stability and strength of the hydrogen bonds.

The RMSD plots and MD interaction fraction histograms of the QA-AR complex are given in Figure 5.

As illustrated in Figure 5A, the average RMSD value for the protein Cα was approximately 2 Å (pale blue), while the average RMSD value for the ligand fitting onto the protein was around 3 Å (red) for over 80% of the simulation time. Additionally, the RMSD value for the ligand itself remained relatively stable at 0.2 Å (pink). Throughout the simulation, various interactions between the ligand and the protein were observed, including hydrogen bonds (green), hydrophobic interactions (purple), ionic interactions (pink), and water bridges (blue).

Figure 5B presents a summary of these interactions using stacked bar charts, with the heights of the bars representing their occurrence frequencies. A value of 0.8 indicates that an interaction is sustained for 80% of the simulation time. Values exceeding 1.0 may occur if certain protein residues engage with the ligand multiple times within the same interaction type. Figure 5B depicts the interaction fractions of the ligand with key residues of the protein over a 100 ns simulation time. The figure also illustrates that specific amino acid residues within the complex are particularly prone to interactions. Notably,

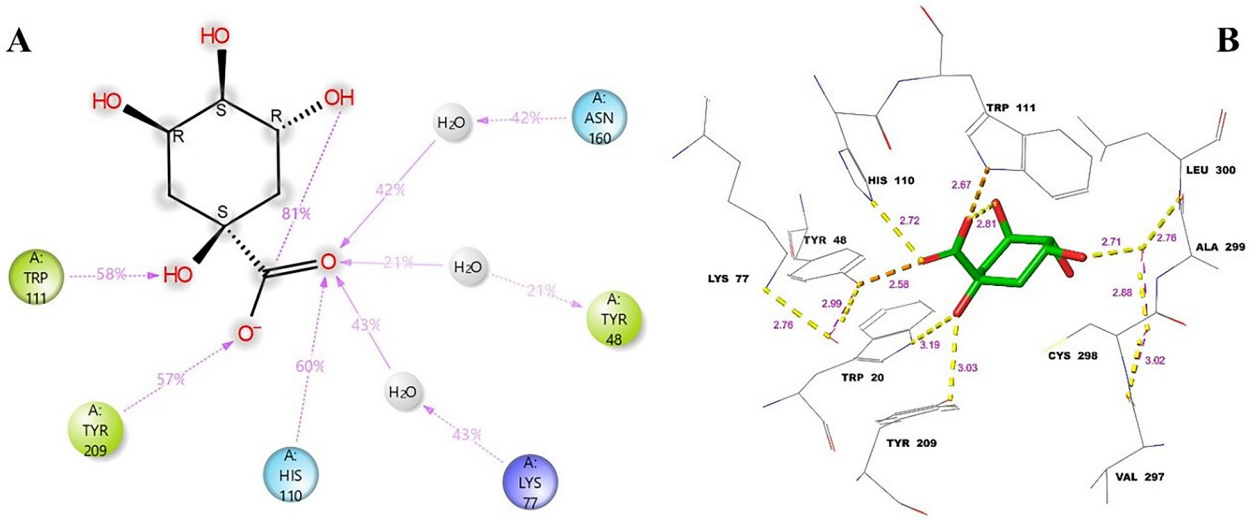

Figure 4. The 2D (A) and 3D (B) key interactions during MD simulation of QA-AR complex

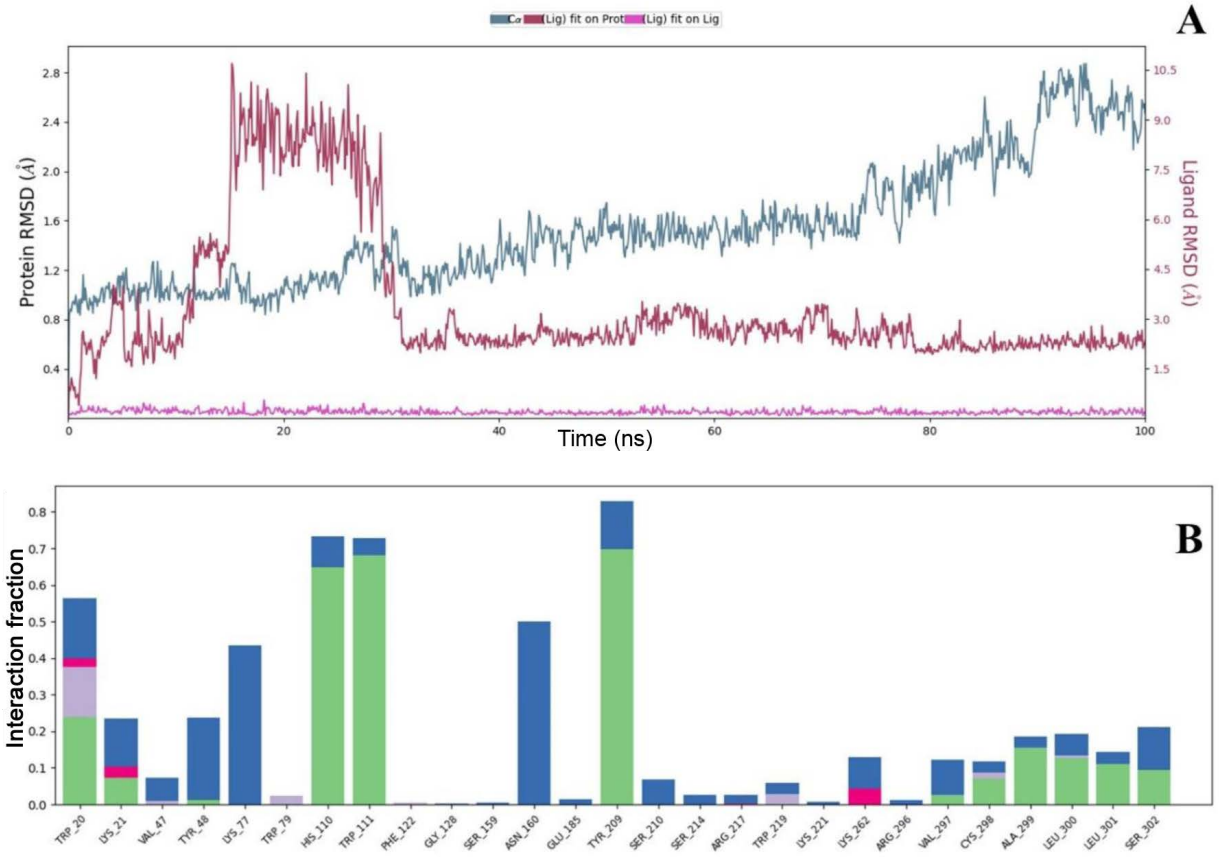

Figure 5. RMSD plots and MD interaction fraction histograms of the QA-AR complex. (A) The left y-axis shows protein Cα RMSD (blue), the right y-axis displays ligand-protein RMSD (red), and the pink line indicates ligand deviation. (B) MD interaction fraction histograms for QA-AR complexes.

Tyr-209 exhibited the most frequent interactions, with a relative abundance exceeding 80%. This suggests that Tyr-209 consistently participates in forming interactions with the ligand throughout the simulation, indicating its crucial role in stabilizing the complex. Similarly, His-110 and Trp-111 demonstrated substantial interaction tendencies, with relative abundances surpassing 70% each. This finding implies that these residues are also integral in forming consistent interactions with the ligand, thereby contributing to the stability and functional dynamics of the complex.

4. Conclusion

In conclusion, this study systematically examined extracts from various components of *Viscum album* L. plants, focusing on their inhibitory effects against the aldose reductase (AR) enzyme. Through comprehensive analyses encompassing both in vitro and in silico approaches, the inhibitory potentials of these extracts were elucidated. Notably, the ethanolic, methanolic, and aqueous extracts derived from different plant parts exhibited varying inhibitory strengths against the AR enzyme, as evidenced by their distinct IC_{50} values. The investigation pinpointed the methanol extract from the stem of *Viscum album* L. as particularly noteworthy, revealing the most potent inhibitory efficacy with an IC_{50} value of 0.156 µM. This potency was attributed to the substantial presence of quinic acid within this extract, supported by its well-established reputation as a robust AR enzyme inhibitor. Moreover, the molecular docking studies provided crucial insights into the binding mechanisms of key compounds, such as chlorogenic acid and fumaric acid, further validating their roles in AR enzyme inhibition. Overall, these findings contribute to a deeper understanding of the potential therapeutic applications of *Viscum album* L. extracts in the context of aldose reductase modulation.

Notes on authors

This study was conducted as part of Bilal AKYÜZ's master's thesis.

Ethical approval statement

This study did not involve any clinical applications, and neither humans nor animals were utilized.

Declaration of interests

The authors declare that they have no competing interests.

References

Adelusi TI, Oyedele A-QK, Boyenle ID, Ogunlana AT, Adeyemi RO et al. (2022). Molecular modeling in drug discovery. Informatics in Medicine Unlocked 29: 100880. https://doi.org/10.1016/j.imu.2022.100880

Akıncıoğlu A, Göksu S, Naderi A, Akıncıoğlu H, Kılınç N et al. (2021). Cholinesterases, carbonic anhydrase inhibitory properties and in silico studies of novel substituted benzylamines derived from dihydrochalcones. Computational Biology and Chemistry 94: 107565. https://doi.org/10.1016/j.compbiolchem.2021.107565

Alim Z, Kilinc N, Sengul B and Beydemir S (2017a). Mechanism of capsaicin inhibition of aldose reductase activity. Journal of Biochemical and Molecular Toxicology 31: e21898. https://doi.org/10.1002/jbt.21898

Alim Z, Kilinç N, Şengül B, Beydemir Ş (2017b). Inhibition behaviours of some phenolic acids on rat kidney aldose reductase enzyme: an in vitro study. Journal of Enzyme Inhibition and Medicinal Chemistry 32: 277-284. https://doi.org/10.1080/14756366.2016.1250752

Apak R, Güçlü K, Özyürek M, Karademir SE (2004). Novel total antioxidant capacity index for dietary polyphenols and vitamins c and e, using their cupric ion reducing capability in the presence of neocuproine: CUPRAC method. Journal of Agricultural and Food Chemistry 52: 7970-7981. https://doi.org/10.1021/jf048741x

Balestri F, Moschini R, Mura U, Cappiello M, Del Corso A (2022). In search of differential inhibitors of aldose reductase. Biomolecules 12: 485. https://doi.org/10.3390/biom12040485

Brand-Williams W, Cuvelier ME, Berset C (1995). Use of a free radical method to evaluate antioxidant activity. LWT - Food Science and Technology 28: 25-30. https://doi.org/10.1016/S0023-6438(95)80008-5

Cerelli MJ, Curtis DL, Dunn JP, Nelson PH, Peak TM et al. (1986). Antiinflammatory and aldose reductase inhibitory activity of some tricyclic arylacetic acids. Journal of Medicinal Chemistry 29: 2347-2351. https://doi.org/10.1021/jm00161a033

Cui C-B, Jeong SK, Lee YS, Lee SO, Kang I-J et al. (2009). Inhibitory activity of caffeoylquinic acids from the aerial parts of Artemisia princes on rat lens aldose reductase and on the formation of advanced glycation end products. Journal of the Korean Society for Applied Biological Chemistry 52: 655-662. https://doi.org/10.3839/jksabc.2009.109

Çakır Ö, Karabulut A (2020). Comparison of two wild-grown Berberis varieties based on biochemical characterization. Journal of Food Processing and Preservation 44: e14844. https://doi.org/10.1111/jfpp.14844

de la Fuente JÁ, Manzanaro S (2003). Aldose reductase inhibitors from natural sources. Natural Product Reports 20: 243-251. https://doi.org/10.1039/B204709H

Ergün F (2021). Determination of antioxidant capacities of mistletoe (*Viscum album* ssp. *austriacum*) leaf and bud extracts. Turkish Journal of Agriculture - Food Science and Technology 9: 2433-2436. https://doi.org/10.24925/turjaf.v9isp.2433-2436.4837

Genheden S, Ryde U (2015). The MM/PBSA and MM/GBSA methods to estimate ligand-binding affinities. Expert Opinion on Drug Discovery 10: 449-461. https://doi.org/10.1517/17460441.2015.1032936

Gök N, Akıncıoğlu A, Erümit Binici E, Akıncıoğlu H, Kılınç N et al. (2021). Synthesis of novel sulfonamides with anti-Alzheimer and antioxidant capacities. Archiv der Pharmazie 354: 2000496. https://doi.org/10.1002/ardp.202000496

Güller U, Güller P, Çiftci M (2021). Radical scavenging and antiacetylcholinesterase activities of ethanolic aextracts of carob, clove, and linden. Alternative Therapies In Health And Medicine 27: 33-37.

Karaaslan EC, 2020. Afyonkarahisar'daki farklı ağaç türleri üzerinde yetişen *Viscum album* L.'un biyolojik özelliklerinin belirlenmesi M.Sc. Thesis, Afyonkarahisar Üniversitesi, Türkiye.

Kılınç N (2021). Inhibition profiles and molecular docking studies of antiproliferative agents against aldose reductase enzyme. International Journal of Chemistry and Technology 5: 77-82. https://doi.org/10.32571/ijct.944049

Kılınç N, Açar M, Tuncay S, Karasakal FÖ (2022a). Potential inhibitors identification of severe acute respiratory syndrome-related coronavirus 2 (SARS-COV-2) angiotensin-converting enzyme 2 and main protease from anatolian traditional plants. Letters in Drug Design & Discovery 19: 996 - 1006. https://doi.org/10.12688/f1000research.52168.2

Kılınç N, Güller U, Alım Z (2022b). Identification of the inhibition effects of some natural antiproliferative agents on ca-i, ca-ii, and ache activities isolated from human erythrocytes by kinetic and molecular docking studies. Russian Journal of Bioorganic Chemistry 48: 720-730. https://doi.org/10.1134/S1068162022040124

Korcan SE, Çankaya N, Azarkan SY, Bulduk İ, Karaaslan EC et al. (2023). Determination of antioxidant activities of *Viscum album* l.: First report on interaction of phenolics with survivin protein using in silico analysis. ChemistrySelect 8: e202300130. https://doi.org/10.1002/slct.202300130

Kousaxidis A, Petrou A, Lavrentaki V, Fesatidou M, Nicolaou I et al. (2020). Aldose reductase and protein tyrosine phosphatase 1B inhibitors as a promising therapeutic approach for diabetes mellitus. European Journal of Medicinal Chemistry 207: 112742. https://doi.org/10.1016/j.ejmech.2020.112742

Köse D, Yiğit fG, Tuncay G, Özcan K (2020). *Viscum album* (ökse otu) ekstrelerinin antimikrobiyal, antioksidan ve antidiyabetik etkilerinin belirlenmesi. Karadeniz Fen Bilimleri Dergisi 10: 380-394. https://doi.org/10.31466/kfbd.808898

Kumlay A, Koçak M, Koyuncu M, Güller U (2021). Bioanalysis of total phenolic contents, volatile compounds, and radical scavenging activities of three wild edible mushrooms. Studia Universitatis Babeş-Bolyai. Chemia 66: 133-148. https://doi.org/10.24193/subbchem.2021.4.10

Orhan DD, Aslan M, Sendogdu N, Ergun F, Yesilada E (2005). Evaluation of the hypoglycemic effect and antioxidant activity of three *Viscum album* subspecies (European mistletoe) in streptozotocin-diabetic rats. Journal of Ethnopharmacology 98: 95-102. https://doi.org/10.1016/j.jep.2004.12.033

Önay E, 2002. Farklı konakçı ağaçlar üzerinde yaşayan ökseotu (*Viscum album* l.) bitkisinde biyokimyasal analizler. Ph.D. Thesis, Fen Bilimleri Enstitüsü, İstanbul Üniversitesi, Türkiye.

ÖnayUçar E, Karagöz A, Arda N (2006). Antioxidant activity of *Viscum album* ssp. album. Fitoterapia 77: 556-560. https://doi.org/10.1016/j.fitote.2006.08.001

Paek JH, Shin KH, Kang Y-H, Lee J-Y, Lim SS (2013). Rapid identification of aldose reductase inhibitory compounds from perilla frutescens. BioMed Research International 2013: 679463. https://doi.org/10.1155/2013/679463

Pietrzak W, Nowak R, Gawlik-Dziki U, Lemieszek MK, Rzeski W (2017). LC-ESI-MS/MS identification of biologically active phenolic compounds in mistletoe berry extracts from different host trees. Molecules 22: 22040624. https://doi.org/10.3390/molecules22040624

Sastry MG, Adzhigirey M, Day T, Annabhimoju R, Sherman W (2013). Protein and ligand preparation: parameters, protocols, and influence on virtual screening enrichments. Journal of Computer-Aided Molecular Design 27: 221-234. https://doi.org/10.1007/s10822-013-9644-8

Singh M, Kapoor A, Bhatnagar A (2021). Physiological and pathological roles of aldose reductase. Metabolites 11: 655. https://doi.org/10.3390/metabo11100655

Slinkard K and Singleton VL (1977). Total phenol analysis: Automation and comparison with manual methods. American Journal of Enology and Viticulture 28: 49. https://doi.org/10.5344/ajev.1977.28.1.49

Şengül B (2023). Evaluation of benzaldehyde derivatives as being bovine kidney aldose reductase inhibitors. Turkish Journal of Nature and Science 12: 61-67. https://doi.org/10.46810/tdfd.1204055

Şengül B, Beydemir Ş (2018). The interactions of cephalosporins on polyol pathway enzymes from sheep kidney. Archives of Physiology and Biochemistry 124: 35-44. https://doi.org/10.1080/13813455.2017.1358749

Şenol H, Ağgül AG and Atasoy S (2023a). Synthesis, characterization, molecular docking and in vitro biological studies of thiazolidin-4-one derivatives as anti-breast-cancer agents. ChemistrySelect 8: e202300481. https://doi.org/10.1002/slct.202300481

Şenol H, Ağgül AG, Atasoy S and Güzeldemirci NU (2023b). Synthesis, characterization, molecular docking and in vitro anti-cancer activity studies of new and highly selective 1,2,3-triazole substituted 4-hydroxybenzohyrdazide derivatives. Journal of Molecular Structure 1283: 135247. https://doi.org/10.1016/j.molstruc.2023.135247

Şenol H, Çağman Z, Katmerlikaya TG, Tokalı FS (2023c). New anthranilic acid hydrazones as fenamate isosteres: Synthesis, characterization, molecular docking, dynamics & in silico adme, in vitro anti-inflammatory and anti-cancer activity studies. Chemistry & Biodiversity 20: e202300773. https://doi.org/10.1002/cbdv.202300773

Şenol H, Ghaffari-Moghaddam M, Bulut Ş, Akbaş F, Köse A et al. (2023d). Synthesis and anticancer activity of novel derivatives of α,β-unsaturated ketones based on oleanolic acid: in vitro and in silico studies against prostate cancer cells. Chemistry & Biodiversity e202301089. https://doi.org/10.1002/cbdv.202301089

Thakur S, Gupta SK, Ali V, Singh P, Verma M (2021). Aldose reductase: a cause and a potential target for the treatment of diabetic complications. Archives of Pharmacal Research 44: 655-667. https://doi.org/10.1007/s12272-021-01343-5

Tokalı FS, Şenol H, Bulut Ş, Hacıosmanoğlu-Aldoğan E (2023a). Synthesis, characterization and molecular docking studies of highly selective new hydrazone derivatives of anthranilic acid and their ring closure analogue Quinazolin-4(3H)-ones against lung cancer cells A549. Journal of Molecular Structure 1282: 135176. https://doi.org/10.1016/j.molstruc.2023.135176

Tokalı FS, Taslimi P, Sadeghi M, Şenol H (2023b). Synthesis and evaluation of quinazolin-4(3H)-one derivatives as multitarget metabolic enzyme inhibitors: A biochemistry-oriented drug design. ChemistrySelect 8: e202301158. https://doi.org/10.1002/slct.202301158

Ullah M, Mehmood S, Khan RA, Ali M, Fozia F et al. (2022). Assessment of antidiabetic potential and phytochemical profiling of viscum album, a traditional antidiabetic plant. Journal of Food Quality 2022: 5691379. https://doi.org/10.1155/2022/5691379

Upadhyay NK, Yogendra Kumar MS, Gupta A (2010). Antioxidant, cytoprotective and antibacterial effects of Sea buckthorn (Hippophae rhamnoides L.) leaves. Food and Chemical Toxicology 48: 3443-3448. https://doi.org/10.1016/j.fct.2010.09.019

Üstüner T (2019). The effects of mistletoe (*Viscum album* L.) on the physiological properties of some drupetrees in Turkey. Turkish Journal of Agriculture and Forestry 43: 485-491. https://doi.org/10.3906/tar-1902-26

Veeresham C, Rama Rao A, Asres K (2014). Aldose reductase inhibitors of plant origin. Phytotherapy Research 28: 317-333. https://doi.org/10.1002/ptr.5000

Yıldız B, Öztürk YE, Kardeş YM, Mut H, Gülümser E (2021). Kaba yem olarak değerlendirilen ökse otunun antioksidan özellikleri ve kondanse tanen İçeriklerinin belirlenmesi. Anadolu Tarım Bilimleri Dergisi 36: 132-137. https://doi.org/10.7161/omuanajas.824020

Yıldız S, Gürgen A, Kılıç C, Tabbouche S, Kılıç AO et al. (2019). Antioxidant, antimicrobial and anti-quorum sensing activities of usnea filipendula and viscum album. Journal of Anatolian Environmental and Animal Sciences 4: 613-620. https://doi.org/10.35229/jaes.636982